ELSEVIER

Journal of Nuclear Materials 318 (2003) 339–347

journal of nuclear materials

www.elsevier.com/locate/jnucmat

Synergy effect of LBE and hydrogenated helium on resistance to LME of T91 steel grade

S. Guerin, J.-L. Pastol, C. Leroux, D. Gorse *

CNRS-CECM, 15 rue Georges Urbain, 94407 Vitry/Seine, France

Abstract

The aim of this paper is to determine the influence of the environment on the resistance to LME of the T91 steel/LBE system. First, we recall that a few hours of exposure to LBE under flowing hydrogenated helium (He–4%H_2) is sufficient to modify the corrosion resistance and wettability of T91 steel, once the temperature attains 350 °C. This result is consistent with a degradation of the protectiveness of the surface oxide film with increasing temperature from 150 to 350 °C, in present experimental conditions. Then, the tensile properties of T91 steel are studied as function of the temperature and cover gas. A reduction in strength and ductility of T91 steel is found, passing through a maximum at the temperature of 350 °C under flowing He–4%H_2, and suggesting a synergy effect of LBE and hydrogenated helium.

1. Introduction

Resistance to embrittlement of 9%Cr martensitic steels in lead–bismuth eutectic (LBE) is a key issue for the future of an experimental X-ADS and specifically of the spallation target modulus, once recalled that today LBE and 9%Cr martensitic steels are the pre-selected structural materials for the liquid metal MEGAPIE spallation target [1–4]. In 1999, in a paper describing the R&D in support of the development of ADS in France, in the frame of the GEDEON program, Salvatores et al. mentioned that liquid metal embrittlement (LME) of 9%Cr martensitic steels should be limited [5]. However, the authors also remarked that the risk of embrittlement of 9%Cr martensitic steels by LBE was nevertheless a matter of concern, and should be examined carefully.

In the present case, it makes the task so complicated because not only is LME per se a tricky problem, but also the solid/liquid system under study is far from the LME model systems for which there is now an abundant experimental and theoretical literature [6–14].

Until now, most of the existing models implicate penetration of 'embrittling species' into grain boundaries (GBs) and give a more or less important role to the (applied or residual) stress and to the deformation state of the solid material. Some authors comment the fact that the crack velocity is often too rapid to be explained by diffusion of embrittling atoms in GBs. Making assumptions on the state (liquid like instead of solid) of the embrittling atoms in the crack tip region and ahead of the crack tip, it is then possible to re-estimate their diffusivity at a level compatible with experimental observations [13]. The more recent models permit to interpret the embrittlement of aluminum alloys by liquid gallium, of copper by liquid bismuth or bismuth alloyed with lead, of nickel by liquid bismuth, with or without applied tensile stress [12–16]. In some cases, the role of the material microstructure on its susceptibility to LME can be at least partially explained [16]. All the above mentioned $metal_{solid}/metal_{liquid}$ (SM/LM) couples are characterized by an easy and rather fast penetration of LM at GBs promoting embrittlement, even at very low or even zero applied stress.

It is worth noticing that SM/LM couples like Fe_{solid}/Pb_{liquid}, $Fe_{solid}/Pb\text{–}Bi_{liquid}$, Cr_{solid}/Pb_{liquid}, Cr_{solid}/Bi_{liquid}

* Corresponding author. Tel.: +33-1 56 70 30 61; fax: +33-1 46 75 04 33.
E-mail address: dominique.gorse@glvt-cnrs.fr (D. Gorse).

0022-3115/03/$ - see front matter © 2003 Elsevier Science B.V. All rights reserved.
doi:10.1016/S0022-3115(03)00081-3

and Fe–Cr solid alloys/LBE are not in the list of the embrittling couples [6–8] and are not known for intergranular penetration of Pb, Bi or LBE and GBs grooving. On the other hand, reduction of strength and ductility of steels under the influence of LBE was reported in a number of Russian papers more than 30 years ago [17,18]. In these papers, first susceptibility to LME is closely associated to the wettability of the steel surface by Pb–Bi and often considered as a direct consequence of the Rebinder effect [19]. Second, the deformation state of the material is emphasized too [10,17]. But we are far from the Al_{solid}/Ga_{liquid} or Cu_{solid}/Bi_{liquid} couples for which both experiments and modeling now exist at same scale.

As concerns Fe–Cr alloys, stressed while in contact with LBE, and before being able to model the available LME observations, one must continue experimental investigations to generate a database related to their resistance to LME and to the correlation 'LME–LMC–Wettability', where LMC refers to liquid metal corrosion.

This justifies the attention paid to the T91 steel/LBE system for which a wide range of experimental parameters must be checked, whatever environmental or metallurgical, in order to assess, at the same time, the embrittling character of this couple and the specific embrittling conditions to be fulfilled. In this paper, we concentrate on the environmental factors susceptible to modify the LME behaviour of the T91 steel/LBE couple. By varying both the oxidation rate and deformation rate of the T91 steel, we determine some experimental conditions leading to the reduction of ductility and energy to rupture of T91 steel, involving a synergy effect of LBE and hydrogenated helium. Attention is paid to the influence of the interfacial oxide film regarding the embrittlement of steels by LBE.

2. Experimental

Tensile specimens (4 mm in diameter and 15 mm in gauge length) are prepared from as-received T91 steel plates provided by Creusot Loire Industrie (CLI), the composition of which is recalled in Table 1. They are submitted to the following standard heat treatment: austenitisation at 1050 °C for 1 h, air quenching, tempering at 750 °C for 1 h and air-cooling. The resulting microstructure is a tempered martensite, with the size of the prior austenitic grains being about 20 μm. Notched specimens are machined to form a V-shaped 60° notch of 0.6 mm in depth and of 0.25 mm root radius in the central part of the specimen gauge length. The LBE alloy ($x_{Pb} = 0.45$ wt%) of 99.99% purity (main impurities: 0.0006%Ag, <0.0003%Te, <0.0001%Ni, <0.0002%Cu, Cd, Sb, Sn, As) supplied by Metaleurop, was purified by HF melting.

In situ tensile tests are performed using a dedicated cell adapted to an electromechanical MTS 20/M machine. The boron nitride coated cell contains 200 ml of LBE either under vacuum or flowing He–4%H_2. Gas circulation begins once the vacuum in the cell is less than 10^{-5} Torr. No oxygen control system is used. The specimens are maintained 12 h in LBE before in situ tensile testing at the aging temperature, fixed between 200 and 400 °C. The rupture facies are examined using a FEG–SEM (LEO 1530) with a zirconia coated tungsten tip. For beam energy as low as 3 keV, the typical resolution was about 3 nm.

3. Results and discussion

3.1. Liquid metal embrittlement: main characteristics and influence of oxide films

We adopt the following definition of LME, stating that putting structural materials under tensile stress into contact with molten low melting metals leads to a reduction in their strength and ductility. LME is essentially considered as one well-established manifestation of the Rebinder effect [19]. Accordingly, LME is based on a reduction of the surface energy (γ_S in inert environment) by adsorption of the atoms of the embrittling molten metallic phase, which reduces the stress required to propagate a crack in accordance with the Griffith theory [20]. For a pre-existing crack of size $2c$, this means that the fracture stress must attain a value $\sigma_C \sim [2E\gamma_{S/L}/\pi c]^{1/2}$ (E is the Young modulus of the solid metal phase) where the solid/liquid interface energy $\gamma_{S/L}$ is used instead of γ_S in inert environment, with $\gamma_{S/L}$ being potentially much lower than γ_S.

A prerequisite of the Rebinder effect is of course perfect wetting of the solid material by the molten metallic phase. This is stated by a number of authors [6–12].

Table 1
Chemical composition of T91 steel (wt%, balance Fe)

C	Mn	P	S	Si	Cr	Mo	Ni
0.105	0.38	0.009	0.003	0.43	8.26	0.95	0.13
V	Nb	N	Al	Cu	As	Sn	Ti
0.2	0.08	0.055	0.024	0.08	0.02	0.008	0.014

In the case of oxidizable alloys, like the 9Cr martensitic steel (T91 steel) studied in this paper, wetting could be obtained:

- Either after removal of the native oxide by ion sputtering and transfer without exposure to air in an UHV chamber to check the resistance to embrittlement of the T91 steel surface wetted by LBE.
- Or after sufficient exposure time of T91 steel in LBE under reducing atmosphere to promote reactivation of the passive surface [21]; no perfect wetting is expected in such case since the steel surface will be roughened after the aging time required for de-oxidation. This is our option in this work, compatible with the experimental set-up previously described [22].

Otherwise, we have to deal with the presence of an oxide film at the T91 steel/LBE interface. However, we make the hypothesis that an embrittling effect can be observed in spite of the presence of an oxide film and that the degree of embrittlement will be strongly dependent on the properties of the oxide film. To our knowledge, there is no experimental proof that an oxide film grown at a SM/LM interface constitutes a barrier against all manifestations of LME. Delayed embrittling effects can be caused by the presence of an oxide film. However it is worth recalling that an oxide film at a SM/LM interface is per se unstable, or at most metastable, depending on its conditions of formation. In fact, the Russians have already treated the influence of oxide films of varying composition on the LME behaviour of some steels in LBE during the 60s. See for example the study of Bichuya concerning the corrosion-fatigue strength of a 1Cr18Ni9Ti steel in LBE [23]. But this gives new thermochemical parameters that one must take into account in order to determine the embrittling conditions for an SM/LM couple.

In 1982, Stoloff reported that the number of combinations of environments and substrates observed to be embrittling couples is constantly expanding as wider test conditions are imposed [11]. Today, this remark is still valid, in the case of all oxidizable metallic alloys with complex microstructures, and also because it is no longer possible to neglect the rather complex properties of the interfacial oxide films that might simply mask or retard a possible embrittling effect.

3.2. Wettability and corrosion resistance of T91 steel in LBE

Wettability and LMC are closely related concepts. To be wetted by a liquid metal, a metal surface can be either 'freshly polished' or covered by an oxide film, provided this film is made unprotective or permeable, due to aging in the corrosive LM phase. Localized or generalized corrosive attack of the steel surface promotes its wettability.

Wettability of T91 steel by lead was studied in the frame of the GEDEON Initiative, with two remarkable results. After ~10 days exposure to stagnant lead at 'high' temperature (~525 °C) under oxygen control, even using highly reducing conditions (~10^{-10} wt O_2), it was not possible to avoid the presence of an oxide film on T91 steel, as revealed by the presence of lead droplets spread at random on the steel surface protected by a $FeCr_2O_4$ film [24]. Three weeks aging under reducing conditions was required to roughen the surface film and induce localized corrosion so as to improve the wettability of T91 steel by lead [21]. At the lower temperature of 380 °C, applying the sessile drop technique to the T91 steel/Pb_{liquid} couple, Lesueur et al. [25] obtained a contact angle of $126 \pm 5°$, remaining constant whatever the annealing time and the volume of the ultra pure lead drop, and suggesting the presence of a passivating oxide layer on T91 steel, under the conditions of the study. More generally, this means that it should always be possible, in principle, to optimize the environmental and aging conditions to favour a direct, at least local T91 steel/Pb_{liquid} contact or conversely to keep passive the steel surface. LBE being known much more corrosive as lead under same operating conditions, the T91 steel surface corrosive attack should be drastically accelerated.

We consider now in parallel the wettability and LMC behaviour of T91 steel after 12 h exposure to stagnant LBE under flowing He–4%H_2 without oxygen control.

Table 2
Corrosion resistance and wettability of T91 steel after short exposure to LBE, without oxygen control, after Pastol et al. [22]

Exposure conditions	Cover gas	Wettability by LBE	Resistance to LMC
12 h at 650 °C	He–4%H_2	Wetting[a]	Locally corroded surface area at macroscopic scale (Fig. 1)
12 h at 600 °C	He–4%H_2	Wetting[a]	No localised corrosion at macroscopic scale (Fig. 1)
1 h at 600 °C + 12 h at 540 °C	He–4%H_2	Wetting[a]	Fe crystallites decorating GB
12 h at 350 °C	He–4%H_2	Toward wetting	Rough and corroded surface only at sub-micrometer scale
12 h at 250 °C	He–4%H_2	No wetting	Passive surface[b]
12 h at 150 °C	He–4%H_2	No wetting	Passive surface[b]

[a] LBE preferentially adherent at inclusions.
[b] At all scales accessible using the FEG–SEM.

The main results are reported in Table 2 and illustrated by Figs. 1 and 2. A priori, we distinguished two temperature ranges: the low temperature range of 150–350 °C, and the elevated one above 600 °C.

We remark a pronounced temperature effect, even in the low temperature range:

- Between 150 and 250 °C, the T91 steel remains passive (Fig. 1(a), left: 150, 250 °C), covered with a thin oxide film whose composition does not vary significantly, according to the EDS spectra of Fig. 1(b). There is no reason to suppose any evolution in the resistance to LMC in these conditions. Apparently, the passivating film prevents wetting by LBE.
- At 350 °C, the change in surface aspect is remarkable at high magnification (Fig. 1(a), right: 350 °C) but already visible at low magnification (Fig. 1(a), left: 350 °C). A porous oxide has grown thick onto the T91 steel. The delamination of the oxide layers has begun after just 12 h of exposure to LBE. The contrast between more or less dark areas (Fig. 1(a), left: 350 °C) could be attributed (at least partially) to oxide layers

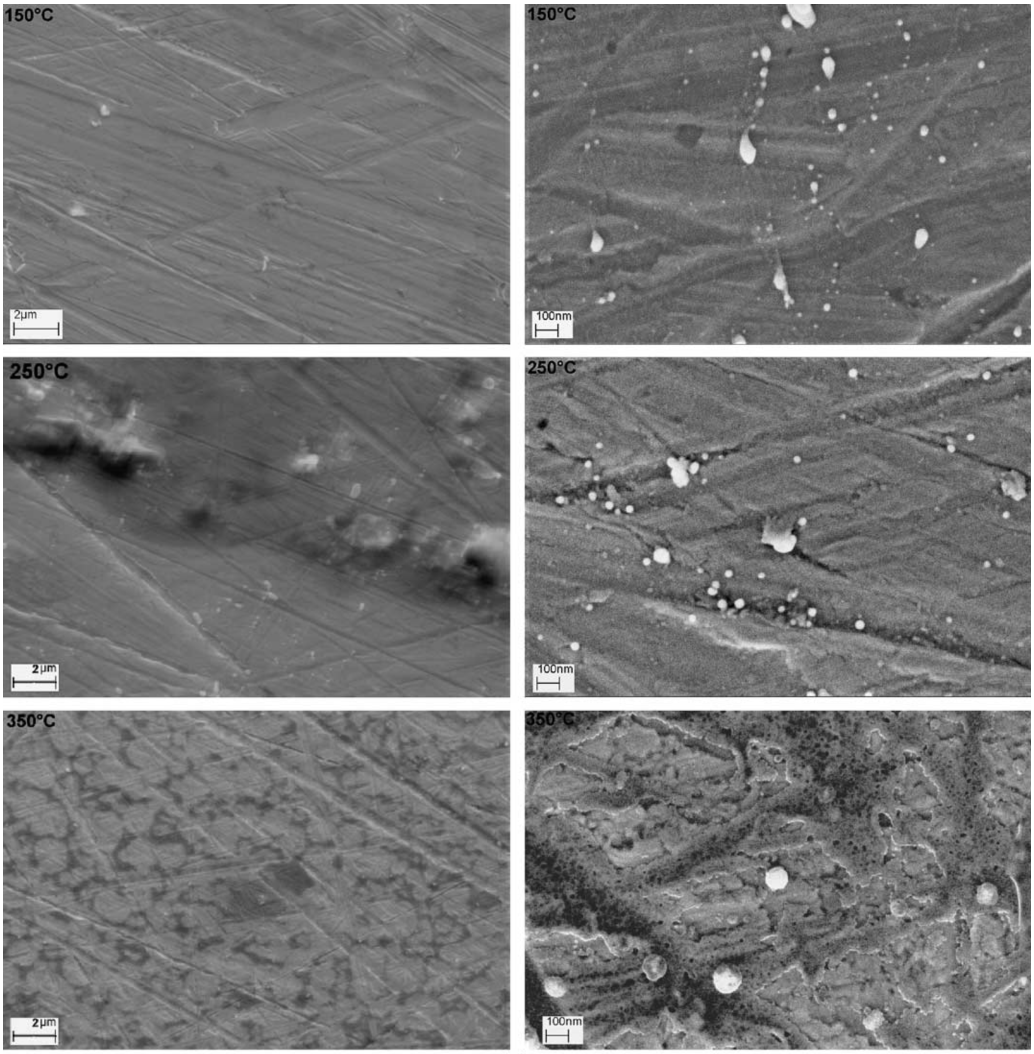

(a)

Fig. 1. (a) SEM micrographs of T91 steel tensile specimens after 12 h exposure to LBE under He–4%H_2 showing the surface states respectively obtained at 150, 250 and 350 °C. The corresponding EDX analysis at 150, 250 and 350 °C are reported in (b). Note the change in the steel surface observed at 350 °C, with delamination of the successive porous oxide layers forming the film. No protectiveness is expected in this case, that could increase the risk of LME. (b) EDX analysis of T91 steel tensile specimens after 12 h exposure to LBE under He–4%H_2, corresponding to the surfaces represented in (a) at respectively 150, 250 and 350 °C. At 350 °C, the two spectra correspond to the two Grey-levels areas of the micrograph at 350 °C (left: low magnification).

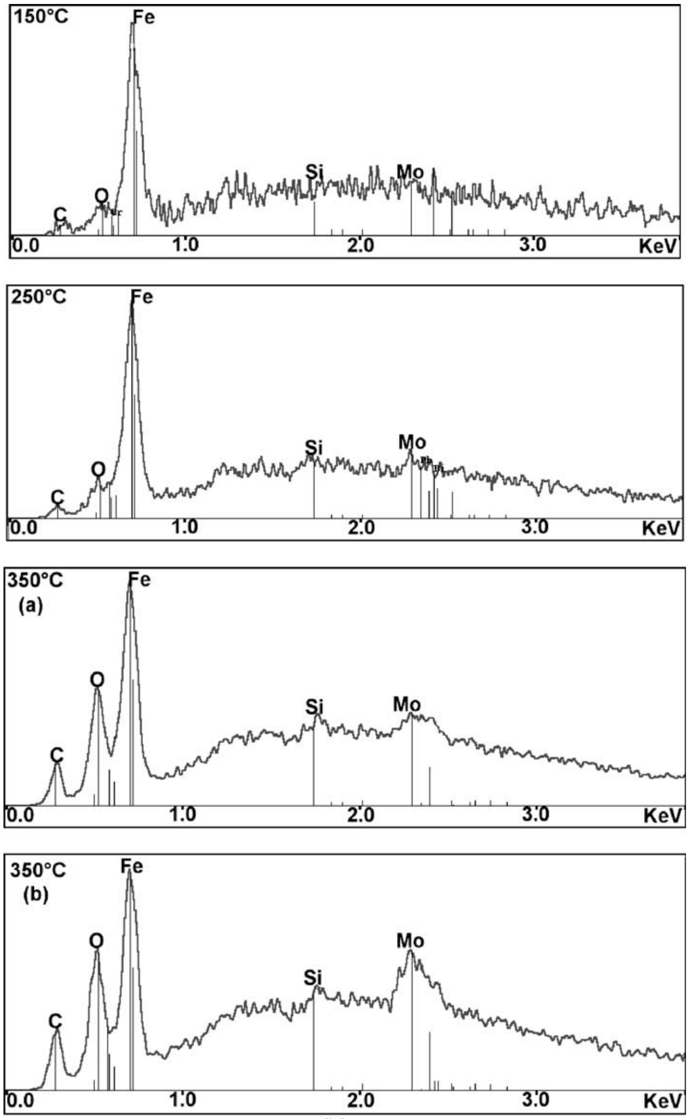

(b)

Fig. 1 (*continued*)

of varying composition (either enriched in silicon or in molybdenum) and porosity, while LBE droplets (~100 nm in size) are retained at the interface within the delaminated region. Consequently, the conditions favorable for wetting are already met at 350 °C.

In the elevated temperature range, at 600–650 °C, the wetting effect is clearly observable at macroscopic scale. Wetting does not proceed uniformly on a steel surface, with inclusions and precipitates (Alumina, nitrides, and carbides ...). They are the preferential nucleation sites for formation of LBE spots adherent to the steel surface. The wetted region increases with increasing temperature, by 'overlap' of localized LBE wetted areas. After 12 h aging at 650 °C, the change in surface morphology is visible at the macroscopic scale, showing both LBE wetted areas and locally corroded (LC) areas (Fig. 2, left: 650 °C). Details of the microstructure of a typical LC area are seen (Fig. 2, right: 650 °C). There is a certain grooving effect of LBE after 12 h at the elevated temperature of 650 °C. We must also note that only in very specific conditions (1 h at 600 °C followed by 12 h at 540 °C) decoration of GBs by iron crystallites was observed with T91 steel [22]. This constitutes the sole indication that LBE, or at least hypothetically bismuth, could penetrate into GBs of the T91 steel.

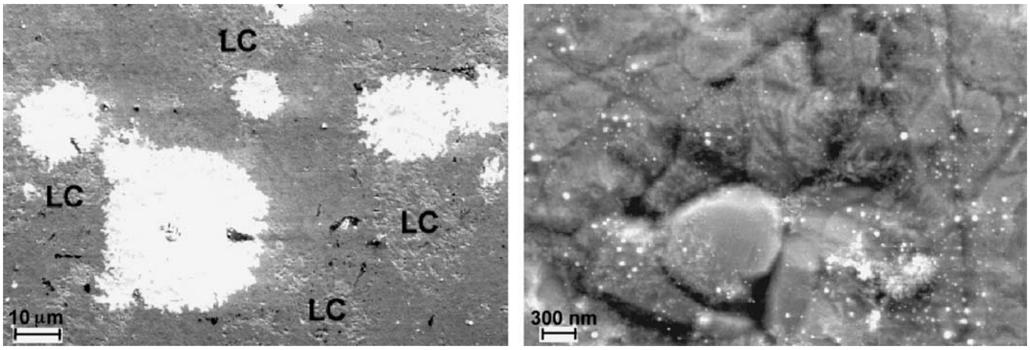

Fig. 2. SEM micrographs of T91 steel tensile specimens after 12 h exposure to LBE at 650 °C under He–4%H_2: (left) revealing both wetted and LC areas, (right) zoom on LC area showing the steel grooving induced by LBE at sub-micrometer scale. Fully deoxidized and facetted zones coexist with well-oxidized ones. After Pastol et al. [22].

From the above mentioned results [22], in the present experimental conditions, it appears that first the native oxide film on T91 steel does not resist to short term exposure to LBE at the high temperature of 650 °C, second that one must keep the temperature of the melt below 350 °C to hinder LMC and wetting effects and maintain the surface passive, at least for short-term aging.

3.3. Tensile behaviour of T91 steel in LBE under vacuum and hydrogenated helium

It was reported previously that there is no difference between the tensile behaviour of T91 steel determined in air at room temperature, without or after 12 h aging in LBE under He–4%H_2 [22]. The delayed fracture observed for a number of systems is not expected here. Except in specific cases where some GB are decorated by Fe crystallites (Table 2), there is no indication that LBE penetrates into T91 steel before crack initiation, as already reported for α-brass wetted with Hg [26]. The concept of intergranular penetration of LBE should not be invoked here, as stated above.

For the T91 steel/LBE couple, the LME effect will depend on both the metallurgical state of the steel and its surface state contacting LBE. This strongly motivates a study of the tensile behaviour as function of the strain rate compared to the corrosion rate. Once attained its critical size, the crack propagation will give rise to the opening of 'fresh' surfaces at crack tip. And one can assume simply that the crack propagation rate will be determined by the competition between the oxidation kinetics in the crack tip area and the kinetics of penetration of the embrittling atoms, once defined the metallurgical conditions (stress–strain state).

In this case, we vary the cross-head displacement rate and the environmental conditions (temperature of LBE and cover gas) to allow for variations of the corrosion rate. The effect of the environment on the tensile behaviour of T91 steel, in absence of any hardening heat treatment, is illustrated with Fig. 3.

Comparing the load versus cross-head displacement curves respectively obtained in vacuum, in LBE under vacuum, under flowing He–4%H_2 and in LBE under flowing He–4%H_2, we remark that both the strength and ductility are altered in all cases with respect to vacuum, but in addition that their reduction depends on both the liquid and gas phase in contact.

As stated above, the steel is protected by its native oxide at the beginning of the tensile test. Few hours in contact with LBE at 350 °C are sufficient to make this film non-protective. On the other hand, the flowing He–4%H_2 cover gas may affect the tensile behaviour due to a change in:

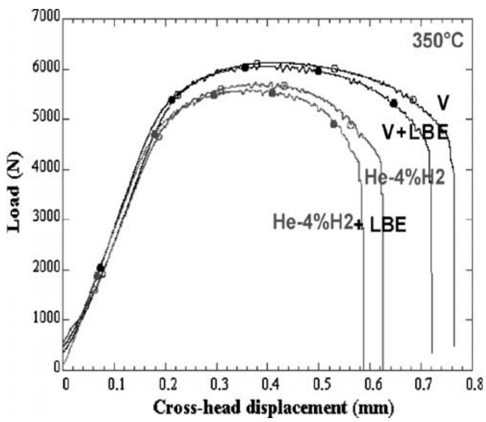

Fig. 3. Load versus cross-head displacement curves obtained with notched T91 steel at 350 °C for a cross-head displacement rate of 6.7 10^{-4} mm/s, showing environmental effects: vacuum (V), LBE under vacuum (V + LBE), He–4%H_2, LBE under He–4%H_2 (He–4%H_2 + LBE).

- Either the surface film by facilitating its rupture and repair, as already known to be a rate determining step of stress corrosion cracking in aqueous media;
- Or also the mechanical properties of T91 steel due to hydrogen ingress, which remains to be proved, at least by varying the hydrogen content in the gas phase.

Last, the degradation of the tensile behaviour is maximized in LBE under flowing He–4%H_2 as a result of a combined and detrimental effect of the liquid and gas phases in contact. It should be too simple to assume that the cover gas by itself allows insuring a good wettability of T91 steel by LBE, sufficient to produce a remarkable LME effect. Indeed, such hypothesis implicates the removal of the native oxide entirely due to flowing He–4%H_2. A synergistic effect of LBE and He–4%H_2 could be invoked to explain the features of Fig. 3.

Changing the environment is one possibility to change the corrosion rate. Doing that at fixed cross-head displacement rate allowed evidencing a certain tendency to LME of the system. To go further, we should examine also the role of temperature for all above mentioned environments and perform the tensile tests over a wide range of 'strain rates'.

A priori, the temperature range of interest should cover the one of the future spallation target windows (200–400 °C). We must also consider the temperature of the MEGAPIE target window now estimated between 330 and 380 °C [27]. Deliberately, we ignore the high temperature LME effects that could occur beyond 600 °C, owing to the severe LMC effects observable at macroscopic scale within the few hours following immersion in LBE (Table 2 and Fig. 2). Based on metallurgic considerations, we should explore the temperature range going from the melting point of LBE up to 550 °C. In the following, we study the intermediate 200–400 °C range. In similar conditions we have shown above that the wettability of T91 by LBE should start at ~350 °C and then increase with increasing temperature.

Thus, the susceptibility to LME is expected to follow the same trend. Accordingly, at 200 °C, no LME effect was detected by means of tensile tests at constant cross-head displacement rate for T91 steel in standard metallurgic state. In Fig. 4, we report the main characteristics of tensile tests carried out with notched specimens for all environments and temperature conditions.

The ductility is defined as the maximum cross-head displacement divided by the initial notch length (0.5 mm). The energy to fracture is calculated as the area under the load versus cross-head displacement curve. Last, the ultimate tensile stress (UTS) is defined as the maximal load divided by the area of the initial notched section (2.8 mm diameter).

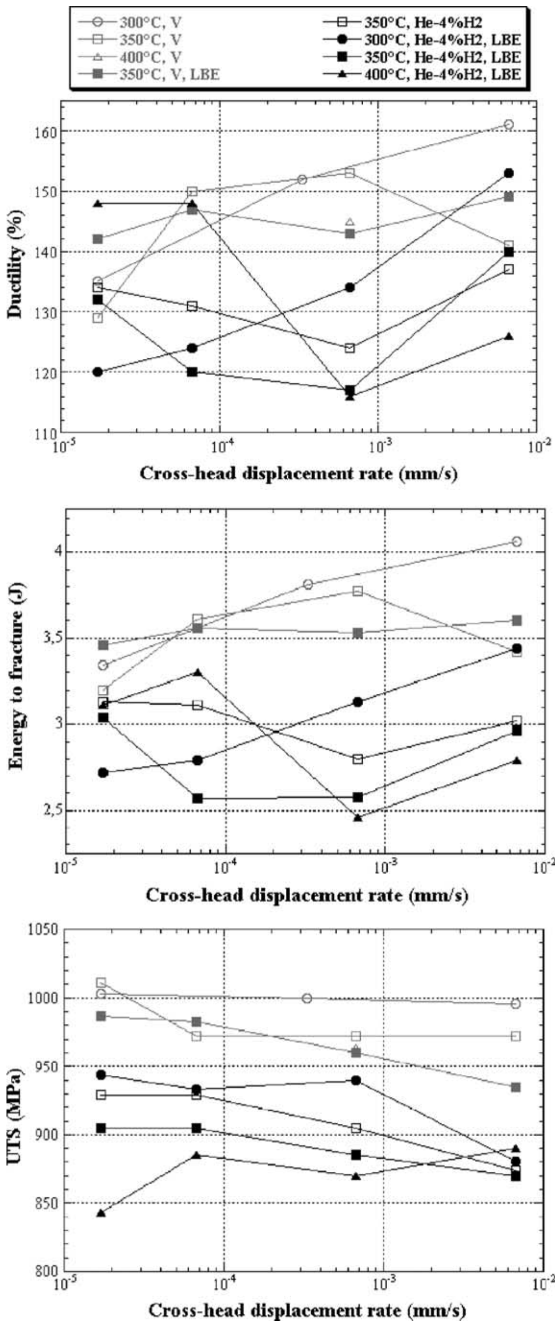

Fig. 4. Ductility, energy to rupture (J) and UTS (MPa) versus cross-head displacement rate obtained with notched T91 steel specimens, showing the conjugated effects of temperature and environment.

There is a LME effect, visible on ductility and energy to fracture (less on UTS), significant in LBE under

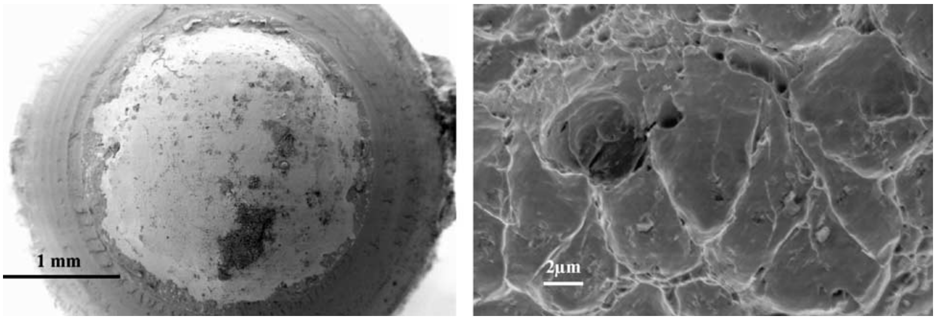

Fig. 5. SEM micrographs of the fracture surface of a notched T91 steel specimen tensioned at a displacement rate of 6×10^{-4} mm/s in LBE under He–4%H_2 cover gas at 350 °C. The fracture surface is completely wetted by LBE (left). The fracture is partially brittle (quasi-cleavage, right).

flowing He–4%H_2, whose importance depends on the deformation rate against oxidation rate.

For 400 °C (▲), at the highest oxidation rate, the ductility trough extends over a narrow range of deformation rates. For 350 °C (■), the ductility trough is bell-shaped and expands over a significant range of deformation rates, whereas for 300 °C (●), one attains only the minimum of ductility for 1.7×10^{-5} mm/s.

Qualitatively, if a crack is initiated at 400 °C for cross-head displacement rates in the range of 10^{-5} mm/s, the oxidation rate is high enough to repassivate the crack and prevent the embrittling effect of LBE before attainment of the critical crack length required for propagation.

To the contrary, when the cross-head displacement rate attains about $\sim10^{-2}$ mm/s, ductile necking is faster than any cracking process.

If one makes the hypothesis that crack initiation is still possible, LBE could not fill the crack sufficiently rapidly, even if an hypothetical crack could be wetted in this case. This interpretation should be valid for the three temperatures, with just a shift in the location of minimum ductility towards slower deformation rates with decreasing temperature to 300 °C, which is observed.

In agreement with the above reasoning, for the cross-head displacement rate of minimum ductility, the fracture surface is generally wetted by LBE. One such exemplary is represented below for a test temperature of 350 °C and a cross-head displacement rate of 6.7×10^{-4} mm/s: the rupture facies still wetted by LBE (Fig. 5, left) is found partially brittle after removal of the adherent molten metal alloy (Fig. 5, right).

4. Conclusions

Once assumed that the T91 steel/LBE system is not prone to intergranular penetration and consequent embrittlement, LME effects (if observable) should depend on both the deformation state of T91 steel and its surface state.

Consequently, a significant part of this paper was dedicated to a study of the wettability and LMC behaviour of T91 steel, in order to determine the evolution of the protectiveness of the surface oxide film, under conditions approaching that of the LME tests:

- At short aging in LBE under flowing He–4%H_2, but without active oxygen control, the native oxide protects the T91 steel against corrosion and is responsible for its poor wettability by LBE, provided the temperature does not exceed 300 °C.
- Beyond, with increasing temperature, and for similar exposure times, the surface film is no longer protective. Delamination of the porous oxide film is observed at microscopic scale once reached 350 °C. In the range of 600–650 °C, LBE causes localized corrosion and wetting initiating preferentially at inclusions sites. In this elevated temperature range, the degradation of the surface state is visible at macroscopic scale.

Tensile tests were then performed under environmental and metallurgical conditions allowing varying the oxidation rate against the deformation rate. A LME effect was found on notched specimens in standard metallurgical state, strongly dependent on the liquid and gas phases in contact. The reduction in strength and ductility, undetectable at 200 °C, passes through a maximum at 350 °C before beginning the ductility recovery at 400 °C. The embrittling influence of LBE is maximized under He–4%H_2, suggesting a synergy effect of LBE and hydrogenated helium.

LME effects after long term exposure to LBE over a wide temperature range are currently investigated. The influence of instabilities of the surface oxide film on the resistance to LME of T91 steel without oxygen control must be understood, before imposing oxygen monitoring.

Acknowledgements

Financial supports from the Chemistry Department of CNRS, from the French Groupement de Recherche GEDEON and from the European Commission in the framework of the TECLA and MEGAPIE-TEST programs are acknowledged. Fruitful discussions with S. Goryachev were appreciated.

References

[1] J.-L. Boutard, D. Gorse, Programme du GDR GEDEON sur les matériaux des Systèmes Hybrides, CEA report ref. DECM 98.078.
[2] Proceedings of the 4th International Workshop on Spallation Materials Technology (IWSMT-4), Schruns, Austria, 8–13 October 2000, J. Nucl. Mater. 296 (2001).
[3] G.S. Bauer, M. Salvatores, G. Heusener, J. Nucl. Mater. 296 (2001) 17.
[4] J.U. Knebel, J.C. Klein, D. Gorse, P. Agostini, F. Gröschel, P. Kupschus, T. Kirchner, J.-B. Vogt, MEGAPIE-TEST: A European project on spallation target testing, American Nuclear Society Winter Meeting, Reno, USA, November 2001.
[5] M. Salvatores, J.-P. Schapira, H. Mouney, B. Carluec, The GEDEON Program, an R&D initiative in support of the ADS development in France, Conf. In Prague, 7–11 June 1999.
[6] W. Rostoker, J.M. McCaughey, H. Markus, Embrittlement by Liquid Metals, Rheinhold, New York, NY, 1960.
[7] M. Kamdar, in: Embrittlement by Liquid Metals, Prog. Mater. Sci., Vol. 15, Pergamon, 1973, p. 289.
[8] F. Shunk, W. Warke, Scr. Metall. 8 (1974) 519.
[9] M. Nicholas, C. Old, J. Mater. Sci. 14 (1979) 1.
[10] V.V. Popovich, Sov. Mater. Sci. 15 (1979) 438.
[11] N.S. Stoloff, in: M.H. Kamdar (Ed.), Embrittlement by Liquid and Solid Metals, The Metallurgical Society of AIME, 1982, p. 3.
[12] B. Joseph, M. Picat, F. Barbier, Eur. Phys. J. AP. 5 (1999) 19.
[13] E. Rabkin, NATO ASI Ser. E 367 (2000) 403.
[14] E. Glickman, NATO ASI Ser. E 367 (2000) 383.
[15] K. Wolski, V. Laporte, N. Marie, M. Biscondi, in: D. Gorse, J.-L. Boutard (Eds.), Proceedings of the International Symposium Structural Materials for Hybrid Systems: a challenge in Metallurgy, J. Phys. IV 12 (2002) Pr8-249.
[16] Y. Brechet, A. Rodine, M. Veron, S. Peron, A. Deschamps, in: D. Gorse, J.-L. Boutard (Eds.), Proceedings of the International Symposium Structural Materials for Hybrid Systems: a challenge in Metallurgy, J. Phys. IV 12 (2002) Pr8-263.
[17] Yu.F. Balandin, I.F. Divisenko, Fiz.-Khim. Mekhan. Mater. 6 (1970) 85.
[18] V.V. Popovich, I.G. Dmukhovskaya, Fiz.-Khim. Mekhan. Mater. 14 (1978) 30.
[19] P.A. Rebinder, in: Anniversary Collection for the 30th year of the Great October Revolution, Part 1, Izd. Akad. Nauk. SSSR, Moscow, 1947, p. 533 (in Russian).
[20] A.A. Griffith, Phil. Trans. R. Soc. A 221 (1921) 163.
[21] F. Gamaoun, M. Dupeux, V. Ghetta, J.-L. Pastol, C. Leroux, S. Guerin, D. Gorse, in: D. Gorse, J.-L. Boutard (Eds.), Proceedings of the International Symposium Structural Materials for Hybrid Systems: a challenge in Metallurgy, J. Phys. IV 12 (2002) Pr8-191.
[22] J.-L. Pastol, P. Plaindoux, C. Leroux, S. Guerin, S. Goryachev, D. Gorse, F. Gamaoun, M. Dupeux, V. Ghetta, in: D. Gorse, J.-L. Boutard (Eds.), Proceedings of the International Symposium Structural Materials for Hybrid Systems: a challenge in Metallurgy, J. Phys. IV 12 (2002) Pr8-203.
[23] A.I. Bichuya, Fiz.-Khim. Mekhan. Mater. 5 (1969) 451.
[24] V. Ghetta, F. Gamaoun, J. Fouletier, M. Hénault, A. Le Moulec, J. Nucl. Mater. 296 (2001) 295.
[25] C. Lesueur, D. Chatain, C. Bergman, P. Gas, F. Baque, in: D. Gorse, J.-L. Boutard (Eds.), Proceedings of the International Symposium Structural Materials for Hybrid Systems: a challenge in Metallurgy, J. Phys. IV, 12 (2002) Pr8-155.
[26] H. Nichols, W. Rostoker, Acta Metall. 8 (1960) 848.
[27] F. Groeschel, Presentation at the MEGAPIE Technical Status Meeting, Bologna, 5–6 March 2002.